



## Can a Bose Gas Be Saturated?

Naaman Tammuz,<sup>1</sup> Robert P. Smith,<sup>1</sup> Robert L. D. Campbell,<sup>1</sup> Scott Beattie,<sup>1</sup> Stuart Moulder,<sup>1</sup>  
Jean Dalibard,<sup>1,2</sup> and Zoran Hadzibabic<sup>1</sup>

<sup>1</sup>*Cavendish Laboratory, University of Cambridge, J. J. Thomson Avenue, Cambridge CB3 0HE, United Kingdom*

<sup>2</sup>*Laboratoire Kastler Brossel, CNRS, UPMC, Ecole Normale Supérieure, 24 rue Lhomond, F-75005 Paris, France*

(Received 25 March 2011; published 6 June 2011)

We scrutinize the concept of saturation of the thermal component in a partially condensed trapped Bose gas. Using a <sup>39</sup>K gas with tunable interactions, we demonstrate strong deviation from Einstein's textbook concept of a saturated vapor. However, the saturation picture can be recovered by extrapolation to the strictly noninteracting limit. We provide evidence for the universality of our observations through additional measurements with a different atomic species, <sup>87</sup>Rb.

DOI: 10.1103/PhysRevLett.106.230401

PACS numbers: 03.75.Hh, 67.85.-d

Bose-Einstein condensation is unique among phase transitions between different states of matter in the sense that it occurs even in the absence of interactions between particles. In Einstein's textbook picture of an ideal gas, purely statistical arguments set an upper bound  $N_c^{(\text{id})}$  on the number of bosons  $N'$  occupying the excited states of the system. Increasing the total number of particles above the critical value  $N_c^{(\text{id})}$  results in saturation of the excited states and macroscopic occupation of the ground state, i.e., Bose-Einstein condensation [1–4].

The condensation observed in weakly interacting, harmonically trapped atomic Bose gases [5–7] is generally believed to provide a faithful illustration of the statistical phase transition proposed by Einstein. In this case, the ideal gas saturation prediction is given by [8]

$$N' \leq N_c^{(\text{id})} = \zeta(3) \left( \frac{k_B T}{\hbar \bar{\omega}} \right)^3, \quad (1)$$

where  $T$  is the temperature,  $\bar{\omega}$  is the geometric mean of the trapping frequencies along the three spatial dimensions, and  $\zeta$  is the Riemann function [ $\zeta(3) \approx 1.202$ ].

However, differences from ideal gas condensation are also observed, for example, in the small deviations of the measured critical atom number  $N_c$  from  $N_c^{(\text{id})}$  [9–11]. In this Letter, we focus on the concept of saturation as the underlying mechanism driving the transition. One might expect that the saturation inequality (1) is essentially satisfied in these systems, with just the value of the bound on the right-hand side slightly modified. We prove that this is far from being the case and show how to reconcile experimental findings with the prediction (1). To do this, we use an ultracold gas of potassium (<sup>39</sup>K) atoms, in which the strength of interactions can be tuned via a Feshbach scattering resonance [12,13].

The crucial step in our work is a proper disentanglement of the subtle role of interactions in condensation. While Einstein's statistical argument does not explicitly invoke interactions between the particles, it does assume that the

gas is in thermal equilibrium, which is fundamentally impossible to attain in a completely noninteracting system [14]. We overcome this problem by making measurements at a range of interaction strengths, always sufficient to ensure thermal equilibrium, and then extrapolating our results to the noninteracting limit, where the saturation picture is recovered.

We perform conceptually simple experiments in which we keep the temperature of the gas constant and vary the atom number. We start with a partially condensed gas of <sup>39</sup>K atoms in the  $|F, m_F\rangle = |1, 1\rangle$  lower hyperfine ground state, produced in a crossed optical dipole trap [16] [see Fig. 1(a)]. The optical potential near the bottom of the trap is close to harmonic, with  $\bar{\omega}/2\pi$  varying between 60 and 80 Hz for data taken at different temperatures. We tune the strength of repulsive interactions in the gas, characterized by the positive  $s$ -wave scattering length  $a$ , by applying a uniform external magnetic field in the vicinity of a Feshbach scattering resonance centered at 402.5 G [17]. We always prepare the condensed gas at  $a = 135a_0$ , where  $a_0$  is the Bohr radius, and then adjust the scattering length to the desired value by changing the applied magnetic field [18]. In a given experimental series, the temperature is kept constant by fixing the depth of our optical trap, and the atom number is varied by holding the gas in the trap for a variable time up to several tens of seconds. During this time the total atom number slowly decays due to three-body recombination, scattering of photons from the trapping laser beams, and collisions with the background gas in the vacuum chamber, while elastic collisions among the trapped atoms ensure equilibrium redistribution of particles between the condensate and the thermal gas [19].

An example of an experimental series, taken at  $a = 135a_0$  and  $T = 177$  nK, is shown in Fig. 1(b). For each hold time between 1 and 110 s, we extract the number of atoms in the condensate,  $N_0$ , and in the thermal gas,  $N'$ , from a bimodal fit to the density distribution of the gas after 18 ms of free time-of-flight expansion from the optical trap [20,21]. We plot  $N_0$  and  $N'$  versus the total number

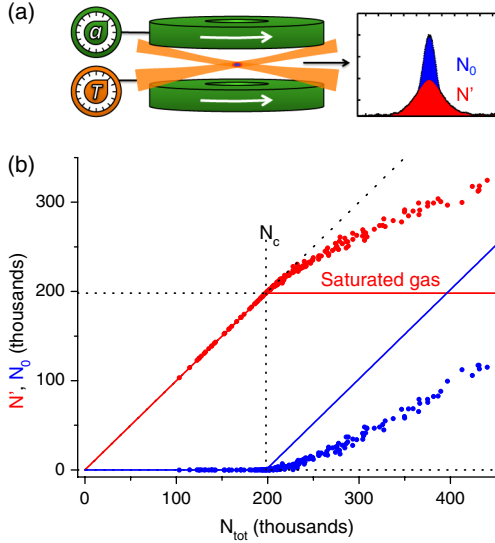


FIG. 1 (color online). Lack of saturation of a Bose gas. (a) Experimental scheme. The temperature  $T$  of a  $^{39}\text{K}$  gas is fixed by the depth of a crossed optical dipole trap, and the scattering length  $a$  is controlled via a Feshbach resonance. The number of thermal ( $N'$ ) and condensed ( $N_0$ ) atoms is extracted from bimodal fits to the density distribution after 18 ms of time-of-flight expansion from the trap. (b)  $N'$  (red points) and  $N_0$  (blue points) versus the total atom number  $N_{\text{tot}}$  at  $T = 177$  nK and  $a = 135a_0$ . The corresponding predictions for a saturated gas are shown by red and blue solid lines. The critical point  $N_{\text{tot}} = N_c$  is marked by a vertical dashed line.

of atoms,  $N_{\text{tot}}$ , which is extracted independently by a direct summation over the density distribution. We find that  $N_{\text{tot}} = N_0 + N'$  is satisfied for all data points to within 0.5%. The standard deviation of the temperature for all the points where the condensate is present is 3 nK [18].

The predictions for the number of condensed and thermal atoms in a saturated gas are shown in Fig. 1(b) by the blue and red solid lines, respectively. Specifically, for  $N_{\text{tot}} > N_c$ , the thermal atom number  $N'$  remains constant and equal to  $N_c$ . The deviation of the experimental data from this prediction is striking. As the total number of atoms is increased from the measured critical value  $N_c \approx 200\,000$  to 450 000, only half of the additional atoms accumulate in the condensate.

In Fig. 2, we show the results of 18 experimental series taken at a wide range of scattering lengths ( $40a_0 < a < 356a_0$ ) and temperatures ( $115 \text{ nK} < T < 284 \text{ nK}$ ). Here we focus on the regime  $N_{\text{tot}} > N_c$ , where the condensate is present, and plot  $N_0$  versus  $N_{\text{tot}} - N_c$ . The solid line shows the prediction for a fully saturated thermal component:  $N_0 = N_{\text{tot}} - N_c$ . The deviation of the data from this prediction is clearly observable in all the series and grows with both  $a$  and  $T$ .

To explore the relationship between the nonsaturation of our Bose gases and the interatomic interactions, we start by identifying the relevant interaction energy. Because of the large ratio between the average densities of the condensed and thermal fractions, the nonideal behavior of the thermal

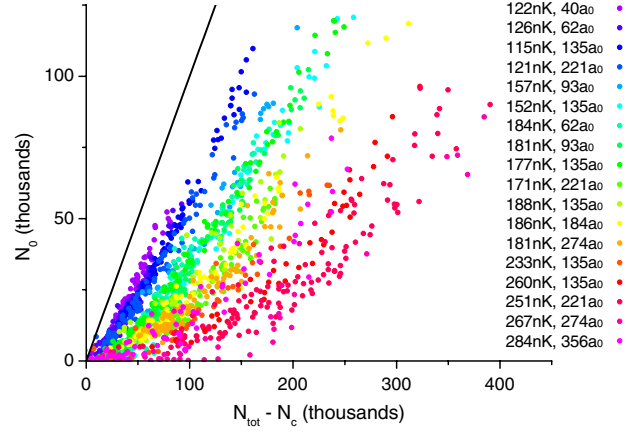


FIG. 2 (color online). Deviation from the saturation picture at a range of interaction strengths and temperatures. We plot  $N_0$  versus  $N_{\text{tot}} - N_c$  for 18 experimental series, each at fixed  $a$  and  $T$ . The values of the scattering length (40–356 $a_0$ ) and the temperature (115–284 nK) are encoded in the color of the data points. The solid line is the prediction for a saturated gas:  $N_0 = N_{\text{tot}} - N_c$ .

component primarily results from its interaction with the condensate. The relevant energy scale is thus [22]

$$\mu_0 = \frac{\hbar\bar{\omega}}{2} \left( 15N_0 \frac{a}{a_{\text{ho}}} \right)^{2/5}, \quad (2)$$

where  $a_{\text{ho}} = (\hbar/m\bar{\omega})^{1/2}$  is the spatial extension of the ground state of the harmonic oscillator of frequency  $\bar{\omega}$  and  $m$  is the atomic mass. The energy  $\mu_0$  is the mean-field prediction for the chemical potential of a gas with  $N_0$  atoms at  $T = 0$  and in the Thomas-Fermi limit [22].

Guided by this scaling, in Fig. 3 we plot the thermal atom number  $N'$  as a function of  $N_0^{2/5}$ , for the same experimental series as shown in Fig. 1(b). From here we proceed in two steps: First, we show that the initial linear increase of  $N'$  with  $N_0^{2/5}$  can be quantitatively accounted for by the mean-field Hartree-Fock (HF) theory for a harmonically trapped gas. Second, for the regime of larger condensates, where the theory does not fully reproduce the experimental data, we adopt a more heuristic approach that still allows us to prove the concept of a saturated gas in the noninteracting limit.

In the HF approach, one treats the thermal fraction as an ideal gas but takes into account repulsive interactions with the condensate. Within this theory [22,23], one gets  $N_c = N_c^{(\text{id})}$  and can predict a linear variation of  $N'/N_c$  with the small parameter  $\mu_0/k_B T$ :

$$\frac{N'}{N_c} = 1 + \alpha \frac{\mu_0}{k_B T}, \quad (3)$$

with  $\alpha = \zeta(2)/\zeta(3) \approx 1.37$  [18]. The origin of this nonsaturation can be understood by noting that interactions with the condensate modify the effective potential seen by the thermal atoms from a parabola into a ‘‘Mexican hat’’

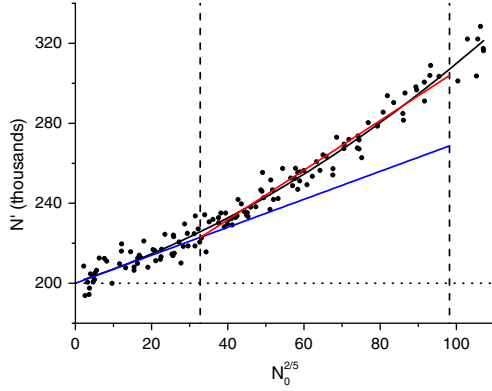


FIG. 3 (color online). Quantifying the lack of saturation. Here  $N'$  is plotted as a function of  $N_0^{2/5}$  for the same series as in Fig. 1(b). The horizontal dotted line is the saturation prediction  $N' = N_c$ . The blue line is the mean-field Hartree-Fock result for a harmonically trapped gas (see the text), with a slope  $S_{\text{HF}} = 699$ . The red line is a linear fit to the data in the range corresponding to  $0.1 < \mu_0/k_B T < 0.3$ , which gives a nonsaturation slope  $S = 1283 \pm 84$ . The solid black line is a guide to the eye based on a second-order polynomial fit. The initial slope of this line is indistinguishable from HF theory.

shape; this allows the thermal component to occupy a larger volume, which grows with increasing  $N_0$  [24].

From Eqs. (2) and (3) we define the nonsaturation slope  $S_{\text{HF}} = dN'/d(N_0^{2/5}) = 1.37X$ , where  $X$  is the dimensionless parameter  $X = \xi T^2 a^{2/5}$ , with  $\xi = 0.5\zeta(3)15^{2/5} (k_B/\hbar\omega)^2 a_{\text{ho}}^{-2/5}$ . The blue line in Fig. 3 corresponds to this prediction, with the intercept fixed by the measured  $N_c$ . It agrees with the data very well for small condensates, with  $N_0 \lesssim 10^4$ , corresponding to  $\mu_0/k_B T \lesssim 0.1$ .

To quantitatively test the prediction of Eq. (3), we took several series at different scattering lengths ( $a = 56\text{--}274a_0$ ) and temperatures ( $T = 177\text{--}317$  nK), specifically focusing on very small values of  $N_0$ . We turn off interactions during time of flight, so that the small condensates almost do not expand and can be reliably detected and characterized in absorption imaging. For each series we fit the initial nonsaturation slope,  $S_0 = dN'/d(N_0^{2/5})$  for  $N_0 \rightarrow 0$ , and compare the result with the prediction  $S_{\text{HF}} = 1.37X$  [26]. As shown in Fig. 4, the experiment and theory agree within a few percent.

The agreement of experiments with Eq. (3) for small  $N_0$  is the first main quantitative result of this Letter and allows us to deduce that the initial nonsaturation slope  $S_0$  would indeed vanish in the noninteracting limit, where  $\mu_0 \rightarrow 0$  for any  $N_0$ . This, however, does not complete our experimental proof, since this theory works very well only for small condensed fractions (see Fig. 3). For the larger, and experimentally more typical, values of  $N_0$ , the nonsaturation of the thermal component is even more pronounced.

To quantitatively study nonsaturation effects at larger  $N_0$ , we take the following heuristic approach: Although the observed increase of  $N'$  with  $N_0^{2/5}$  is not perfectly linear,

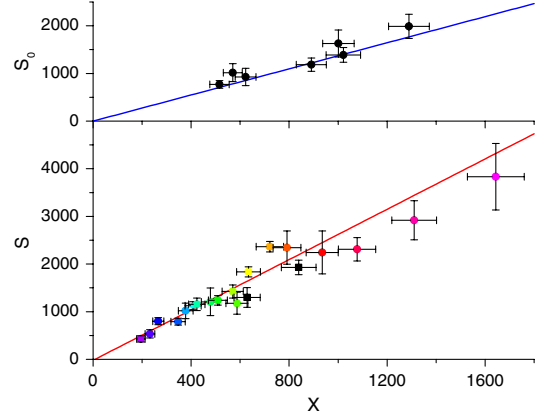


FIG. 4 (color online). Saturation in the noninteracting limit. The nonsaturation slopes  $S_0$  and  $S$  are plotted versus the dimensionless parameter  $X = \xi T^2 a^{2/5}$  (see the text). The  $S_0$  data are directly compared with Hartree-Fock theory,  $S_{\text{HF}} = 1.37X$  (blue line), with no free parameters. For the  $S$  data, a linear fit (red line) gives  $dS/dX = 2.6 \pm 0.3$  and an intercept  $S(0) = -20 \pm 100$ , consistent with complete saturation in the ideal gas limit. The  $S$  data are based on the 18  $^{39}\text{K}$  series shown with the same symbol code in Fig. 2 and two additional series taken with  $^{87}\text{Rb}$  (black squares). All vertical error bars are statistical. The systematic uncertainty in atom numbers  $N'$  and  $N_0$  is  $<10\%$ , corresponding to  $<6\%$  uncertainty in  $S_0$  and  $S$  values. The horizontal error bars include the 3 Hz uncertainty in the trapping frequencies  $\bar{\omega}/2\pi$  and (for potassium) the 0.1 G uncertainty in the position of the Feshbach resonance.

over a broad experimentally relevant range it can be well quantified by a coarse-grained slope  $S = \Delta[N']/\Delta[N_0^{2/5}]$ , as indicated in Fig. 3 by the red solid line. In order to treat all the data taken at various values of  $a$  and  $T$  equally, for each experimental series we consider the same range of values of  $\mu_0/k_B T$ , from 0.1 to 0.3. Note that this range covers more than an order of magnitude of  $N_0$  values and encompasses the bulk of the data shown in Fig. 2 [27].

In Fig. 4, we summarize the nonsaturation slopes  $S(a, T)$  for the same 18 experimental series shown in Fig. 2. Within experimental error, all data points fall onto a straight line when plotted against the dimensionless parameter  $X = \xi T^2 a^{2/5}$ , supporting the assumption that we can still use  $\mu_0/k_B T$  as the relevant interaction parameter. To further validate our approach, we took additional data with a different atomic species,  $^{87}\text{Rb}$ , in the  $|F, m_F\rangle = |2, 2\rangle$  state. In this case  $a = 99a_0$  is not tunable, and the two experimental series were taken at  $T = 175$  and  $T = 203$  nK. These two points are in close agreement with the  $^{39}\text{K}$  data.

The prediction (1) for an ideal gas ( $a = 0$ ) corresponds to  $S = 0$  at the origin of the graph in Fig. 4. The mathematical limit  $X \rightarrow 0$  is reached in two physically very different limits:  $a \rightarrow 0$  and  $T \rightarrow 0$ . In the mundane  $T \rightarrow 0$  limit,  $N'$  inevitably vanishes for any value of  $N_0$ , so trivially  $S = 0$ . It is therefore essential that our experiments show that  $S$  depends only on the parameter  $X \propto T^2 a^{2/5}$ , allowing us to deduce its value in the  $a \rightarrow 0$

limit for any fixed  $T$ . The solid line in Fig. 4 shows the result of an unconstrained linear fit to the data, which gives an intercept consistent with zero:  $S(0) = -20 \pm 100$ . Together with the success of HF theory in the small  $N_0$  regime, this confirms the concept of a saturated Bose gas for a broad range of experimentally relevant parameters.

We expect our results to be generic to experiments on harmonically trapped 3D Bose gases with (relatively weak) short-range  $s$ -wave interactions. However, a number of important questions remain open. Here we studied only the global properties of the gas, inferred from the number of atoms in condensed and thermal components; in the future, it would be of great interest to also study saturation at the level of local densities of the two components and effectively measure the equation of state for a bulk system [28]. Local saturation should depend only on the interactions between particles but could, for example, be different in systems with very strong or long-range interactions, where the emergence of a roton minimum significantly increases the density of states for low energy excitations. Global saturation additionally depends on the external potential, and from purely geometric arguments we expect the nonsaturation effects to grow with the dimensionality of the system. In this respect it would be particularly interesting to study them for atomic gases in disordered potentials [29], where the possible fractal nature of the fluid shape can lead to a noninteger effective dimensionality.

In conclusion, our work shows that the purely statistical picture of a saturated Bose gas is not realized in experiments with harmonically trapped atomic vapors. However, extrapolation of our results to the strictly noninteracting limit allows us to confirm the textbook picture of Bose-Einstein condensation as a purely statistical phase transition in an ideal gas. Ultracold atomic gases offer great experimental flexibility for further studies of (non)saturation effects, which may provide a fruitful way of classifying different geometries and interactions in many-body systems.

We thank P. Krüger and D. Hutchinson for useful discussions and N. Cooper, F. Gerbier, M. Köhl, and C. Salomon for helpful comments on the manuscript. This work was supported by EPSRC (Grants No. EP/G026823/1 and No. EP/I010580/1). R. P. S. acknowledges support from the Newton Trust. J. D. acknowledges hospitality of the Cavendish Lab and Trinity College, Cambridge.

- 
- [1] A. Einstein, *Sitzungsber. Preuss. Akad. Wiss. Phys. Math. Kl.*, 3 (1925).
  - [2] K. Huang, *Statistical Mechanics* (Wiley, New York, 1987).
  - [3] C. Pethick and H. Smith, *Bose-Einstein Condensation in Dilute Gases* (Cambridge University Press, Cambridge, England, 2002).
  - [4] L. Pitaevskii and S. Stringari, *Bose-Einstein Condensation* (Oxford University, New York, 2003).
  - [5] M. H. Anderson *et al.*, *Science* **269**, 198 (1995).
  - [6] K. B. Davis *et al.*, *Phys. Rev. Lett.* **75**, 3969 (1995).

- [7] C. C. Bradley, C. A. Sackett, and R. G. Hulet, *Phys. Rev. Lett.* **78**, 985 (1997).
- [8] V. Bagnato, D. E. Pritchard, and D. Kleppner, *Phys. Rev. A* **35**, 4354 (1987).
- [9] J. R. Ensher *et al.*, *Phys. Rev. Lett.* **77**, 4984 (1996).
- [10] F. Gerbier *et al.*, *Phys. Rev. Lett.* **92**, 030405 (2004).
- [11] R. Meppelink *et al.*, *Phys. Rev. A* **81**, 053632 (2010).
- [12] G. Roati *et al.*, *Phys. Rev. Lett.* **99**, 010403 (2007).
- [13] C. Chin, R. Grimm, P. Julienne, and E. Tiesinga, *Rev. Mod. Phys.* **82**, 1225 (2010).
- [14] In the recently observed Bose-Einstein condensation of a photon gas [15], there is no direct interaction between the light particles. However, the interaction with the material environment, which ensures thermalization, leads to a second-order interaction between the photons. The resulting nonsaturation of the gas is visible in Fig. 2 of Ref. [15].
- [15] J. Klaers, J. Schmitt, F. Vewinger, and M. Weitz, *Nature (London)* **468**, 545 (2010).
- [16] R. L. D. Campbell *et al.*, *Phys. Rev. A* **82**, 063611 (2010).
- [17] M. Zaccanti *et al.*, *Nature Phys.* **5**, 586 (2009).
- [18] See supplemental material at <http://link.aps.org/supplemental/10.1103/PhysRevLett.106.230401> for more details.
- [19] Heating due to density-dependent three-body recombination is compensated by residual evaporation in a finite-depth trap. Since the thermalization rate is much higher than the atom-loss rate, the details of the loss mechanism do not affect the quasistatic thermodynamic properties of the gas.
- [20] W. Ketterle, D. S. Durfee, and D. M. Stamper-Kurn, in *Bose-Einstein Condensation in Atomic Gases*, Proceedings of the International School of Physics Enrico Fermi, Course CXL, edited by M. Inguscio, S. Stringari, and C. Wieman (IOS Press, Amsterdam, 1999), p. 67.
- [21] F. Gerbier *et al.*, *Phys. Rev. A* **70**, 013607 (2004).
- [22] F. Dalfovo, S. Giorgini, L. P. Pitaevskii, and S. Stringari, *Rev. Mod. Phys.* **71**, 463 (1999).
- [23] S. Giorgini, L. P. Pitaevskii, and S. Stringari, *J. Low Temp. Phys.* **109**, 309 (1997).
- [24] In Ref. [25], condensation was studied in a spinor gas, where atoms were gradually transferred from condensed spin components into an initially unpopulated one. The thermal atoms thus experienced a potential modified by interactions with the already existing condensates, which probably obscured the differential nonsaturation effects due to the newly emerging condensate.
- [25] M. Erhard *et al.*, *Phys. Rev. A* **70**, 031602 (2004).
- [26] We analytically correct for small temperature variations within a series by using the scaling given by the HF theory. This amounts to plotting  $N'(T/T')^3$  versus  $N_0^{2/5}(T/T')$ , where  $T'$  is assigned to each data point and  $T$  is the nominal temperature for a series, obtained in the  $N_0 \rightarrow 0$  limit.
- [27] The data shown in Fig. 3 can also be described by a second-order polynomial fit, instead of using the two slopes  $S_0$  and  $S$ . However, this relies on precise measurements at very low  $N_0$ , which are often not available. For this reason, a single empirically defined parameter  $S$  is more useful for describing typical experiments, over the typical range of  $N_0$  values.
- [28] T.-L. Ho and Q. Zhou, *Nature Phys.* **6**, 131 (2010).
- [29] L. Sanchez-Palencia and M. Lewenstein, *Nature Phys.* **6**, 87 (2010).